

U.S. DEPARTMENT OF COMMERCE  
National Technical Information Service

AD-A031 590

EFFECT OF MULTIPATH ON THE HEIGHT-FINDING  
CAPABILITY OF FIXED-REFLECTOR RADAR SYSTEMS  
PART 2. APPLICATION TO AN AIR SEARCH  
RADAR SYSTEM

ROME AIR DEVELOPMENT CENTER,  
GRIFFISS AIR FORCE BASE, NEW YORK

JULY 1976

313114

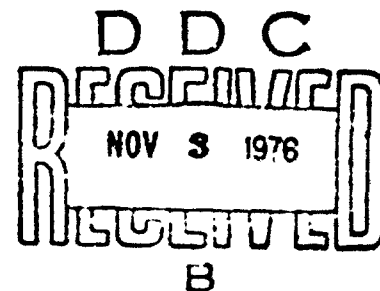
AD A031590

RADC-TR-76-215  
BRIEFING REPORT  
JULY 1976



# Effect of Multipath on the Height-Finding Capability of Fixed-Reflector Radar Systems Part 2: Application to an Air Search Radar System

RONALD L. FANTE  
PETER R. FRANCHI  
RICHARD L. TAYLOR



Approved for public release; distribution unlimited.

ROME AIR DEVELOPMENT CENTER  
AIR FORCE SYSTEMS COMMAND  
GRIFFISS AIR FORCE BASE, NEW YORK 13441

PUBLICATION REVIEW

This report has been reviewed by the RADC Information Office (OI) and is releasable to the National Technical Information Service (NTIS). At NTIS it will be releasable to the general public, including foreign nations.

APPROVED: *Walter Rotman*  
WALTER ROTMAN, Chief  
Microwave Detection Techniques Br.

APPROVED: *Walter Rotman*  
WALTER ROTMAN, Acting Chief  
Electromagnetic Sciences Division

ACCESSION BY	
NTIS	White Section <input checked="" type="checkbox"/>
DDC	Ref. Section <input type="checkbox"/>
UNANNOUNCED	<input type="checkbox"/>
JUSTIFICATION	
BY	
DISTRIBUTION/AVAILABILITY CODES	
Dist.	AVAIL. and/or SPECIAL
A	

FOR THE COMMANDER:

*John B. Hues*

Plans Office

Unclassified

SECURITY CLASSIFICATION OF THIS PAGE (When Data Entered)

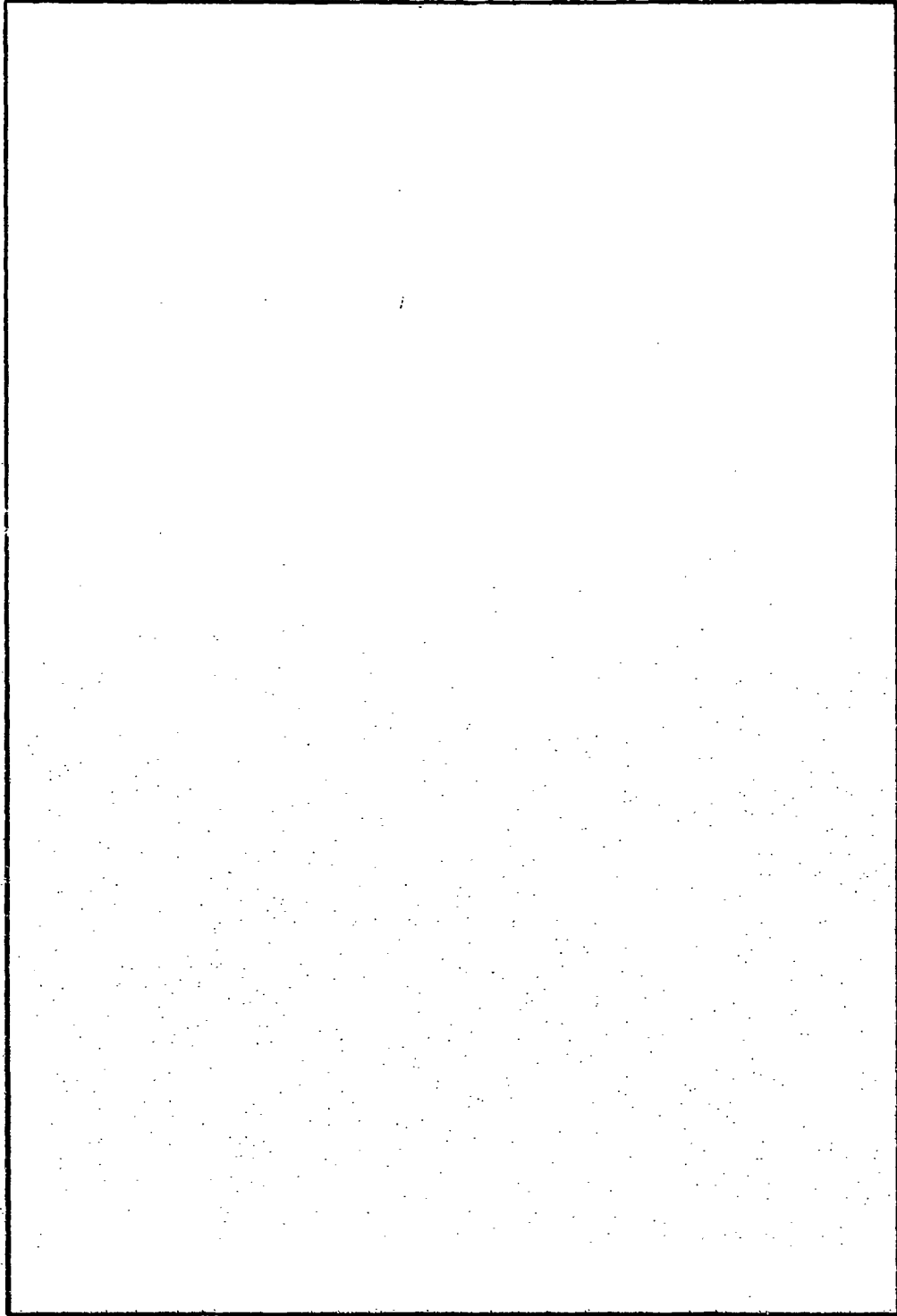
REPORT DOCUMENTATION PAGE		READ INSTRUCTIONS BEFORE COMPLETING FORM
1. REPORT NUMBER RADC-TR-76-215	2. GOVT ACCESSION NO.	3. RECIPIENT'S CATALOG NUMBER
4. TITLE (and Subtitle) EFFECT OF MULTIPATH ON THE HEIGHT-FINDING CAPABILITY OF FIXED-REFLECTOR RADAR SYSTEMS, PART 2: APPLICATION TO AN AIR SEARCH RADAR SYSTEM		5. TYPE OF REPORT & PERIOD COVERED In-House.
7. AUTHOR(s) Ronald L. Fante Peter R. Franchi Richard L. Taylor		8. CONTRACT OR GRANT NUMBER(s)
9. PERFORMING ORGANIZATION NAME AND ADDRESS Deputy for Electronic Technology (RADC/EETP) Hanscom AFB, Massachusetts 01731		10. PROGRAM ELEMENT, PROJECT, TASK AND WORK UNIT NUMBERS 61102F 21530201
11. CONTROLLING OFFICE NAME AND ADDRESS Deputy for Electronic Technology (RADC/EETP) Hanscom AFB, Massachusetts 01731		12. REPORT DATE July 1976
14. MONITORING AGENCY NAME & ADDRESS (if different from Controlling Office)		13. NUMBER OF PAGES 27
		15. SECURITY CLASS. (of this report) Unclassified
		15a. DECLASSIFICATION/DOWNGRADING SCHEDULE
16. DISTRIBUTION STATEMENT (of this Report) Approved for public release; distribution unlimited.		
17. DISTRIBUTION STATEMENT (of the abstract entered in Block 20, if different from Report)		
18. SUPPLEMENTARY NOTES		
19. KEY WORDS (Continue on reverse side if necessary and identify by block number) Radar Reflector antennas		
20. ABSTRACT (Continue on reverse side if necessary and identify by block number) The errors due to multipath in target altitude for a modified air search radar system have been evaluated. A method for decreasing these altitude errors has been discussed and evaluated.		

FORM 1473 EDITION OF 1 NOV 68 IS OBSOLETE

Unclassified  
SECURITY CLASSIFICATION OF THIS PAGE (When Data Entered)

Unclassified

SECURITY CLASSIFICATION OF THIS PAGE(When Data Entered)



Unclassified

SECURITY CLASSIFICATION OF THIS PAGE(When Data Entered)

## Contents

1. INTRODUCTION	7
2. THEORETICAL REVIEW	7
3. SINGLE-HIT ERRORS	11
4. MULTIPLE-HIT ERRORS	18
5. CONCLUSIONS	20
APPENDIX A: Element Pattern	21
APPENDIX B: Radiation Patterns for Various Types and Locations of the Secondary Horn	23
APPENDIX C: Altitude Error Plots	25

## Illustrations

1. Modification of a Reflector Antenna so as to Obtain Altitude Information	8
2. Geometry of the Direct and Multipath Links	9
3. Maximum Altitude Error for Reflector Elevation, $d = 0.05$ miles and Target Range, $R = 50$ miles	13
4. Maximum Altitude Error for Reflector Elevation, $d = 0.05$ miles and Target Range, $R = 100$ miles	13

## Illustrations

5.	Maximum Altitude Error for Reflector Elevation, $d = 0.05$ Miles and Target Range, $R = 150$ Miles	14
6.	Maximum Altitude Error for Reflector Elevation, $d = 0.05$ Miles and Target Range, $R = 200$ Miles	14
7.	Phase Angle of the Radiation Field for the Primary Horn ( $\phi_0$ ) and the Secondary Horn ( $\phi_1$ ) for the Conditions of Case D of Table 1	15
8.	Effects of Using the Incorrect Assumption $\psi_1 = \psi_2$ on the Maximum Altitude Error for the Reflector of Case A (Table 1) and $R = 100$ Miles, $d = 0.05$ Miles	16
9.	Effect of Using the Incorrect Assumption $\psi_1 = \psi_2$ on the Maximum Altitude Error for the Reflector of Case A (Table 1) and $R = 150$ Miles, $d = 0.05$ Miles	16
10.	Effect of Using the Incorrect Assumption $\psi_1 = \psi_2$ on the Maximum Altitude Error for the Reflector of Case D (Table 1) and $R = 100$ Miles, $d = 0.05$ Miles	17
11.	Effect of Using the Incorrect Assumption $\psi_1 = \psi_2$ on the Maximum Altitude Error for the Reflector of Case D (Table 1) and $R = 150$ Miles, $d = 0.05$ Miles	17
12.	Effect of Averaging on the Maximum Altitude Error for a Target Flying at 3 Miles Altitude, for Case C of Table 1	19
13.	Effect of Averaging on the Maximum Altitude Error for a Target Flying at 6 Miles Altitude, for Case C of Table 1	20
A1.	Radiation Pattern for the Reflector for the Case When the Primary Horn is Located at $x_0 = -34.0$ , $y_0 = 0$ , $z_0 = 202.830$	22
B1.	Radiation Pattern When the Secondary Horn is Located at $x_1 = 51.47^\circ$ , $z_1 = 201.15^\circ$ and has $F(\psi_1) = 1 - 4.92\psi_1^2$ (denoted by Case A in Table 1)	24
B2.	Radiation Pattern When the Secondary Horn is Located at $x_1 = 57.43^\circ$ , $z_1 = 200.32^\circ$ and has $F(\psi_1) = \exp(-18.05\psi_1^2)$ , (denoted by Case B in Table 1)	24
B3.	Radiation Pattern When the Secondary Horn is Located at $x_1 = -51.47^\circ$ , $z_1 = 201.15^\circ$ and has $F(\psi_1) = \exp(-18.05\psi_1^2)$ , (denoted by Case C in Table 1)	24
B4.	Radiation Pattern When the Secondary Horn is Located at $x_1 = .55.63^\circ$ , $z_1 = 200.580^\circ$ and has $F(\psi_1) = 1.0$ (denoted by Case D in Table 1)	24
C1.	Altitude Error (miles) vs Altitude (miles) for a Target Range of 100 Miles	26
C2.	Altitude Error (miles) vs Altitude (miles) for 100 Mile Target Range	26
C3.	Altitude Error (miles) vs Altitude (miles) for 150 Mile Target Range	26
C4.	Altitude Error (miles) vs Altitude (miles) for 150 Mile Target Range	26
C5.	Altitude Error (miles) vs Range (miles) for a Target Altitude of 3 Miles and Reflector Elevation $d = 0.01$ Miles (52')	27
C6.	Altitude Error (miles) vs Range (miles) for a Target Altitude of 6 Miles and a Reflector Elevation $d = 0.01$ Miles (52') Assuming the Reflector System of Case C in Table 1	27

## Illustrations

- |   |    |
|---|----|
| C7. Altitude Error (miles) vs Range (miles) for a Target Altitude of 3 Miles and a Reflector Elevation $d = 0.76$ Miles (4000'), Assuming the Reflector System of Case C in Table 1 | 27 |
| C8. Altitude Error (miles) vs Range (miles) for a Target Altitude of 6 Miles and a Reflector Elevation $d = 0.76$ Miles (4000'), Assuming the Reflector System of Case C in Table 1 | 27 |

## Tables

- |   |    |
|---|----|
| 1. Location and Pattern of the Secondary Horn   | 12 |
| 2. Relationship Between Altitude $H$ and $\theta$ for a Spherical Earth, and $d = 0.05$ Miles | 15 |

# Effect of Multipath on the Height-Finding Capability of Fixed-Reflector Radar Systems Part 2: Application to an Air Search Radar System

## 1. INTRODUCTION

In Part 1 of this report we developed the theory necessary for determining the error (due to multipath) in the altitude measuring capability of a reflector radar which is modified so as to operate in a monopulse mode. In this portion we will present detailed calculations specifically for an air search radar system, which is modified by adding a second feed horn, and then operated as a monopulse system, as is indicated in Figure 1.

## 2. THEORETICAL REVIEW

Before going on to present results for the altitude errors due to multipath, we shall first discuss the operation of the modified air search radar when multipath is absent. Let us consider the reflector in Figure 1 and assume that in the absence of multipath the far-field pattern due to the primary horn is  $f_0(\theta) \exp \{i \phi_0(\theta)\}$  where  $\theta$  is the elevation angle and  $f_0(\theta)$  is real. Also assume that in the absence of multipath the far-field pattern due to secondary horn is  $f_1(\theta) \exp \{i \phi_1(\theta)\}$ . Then the output voltage of the log amplifiers in Figure 1 is

---

(Received for publication 16 July 1976)

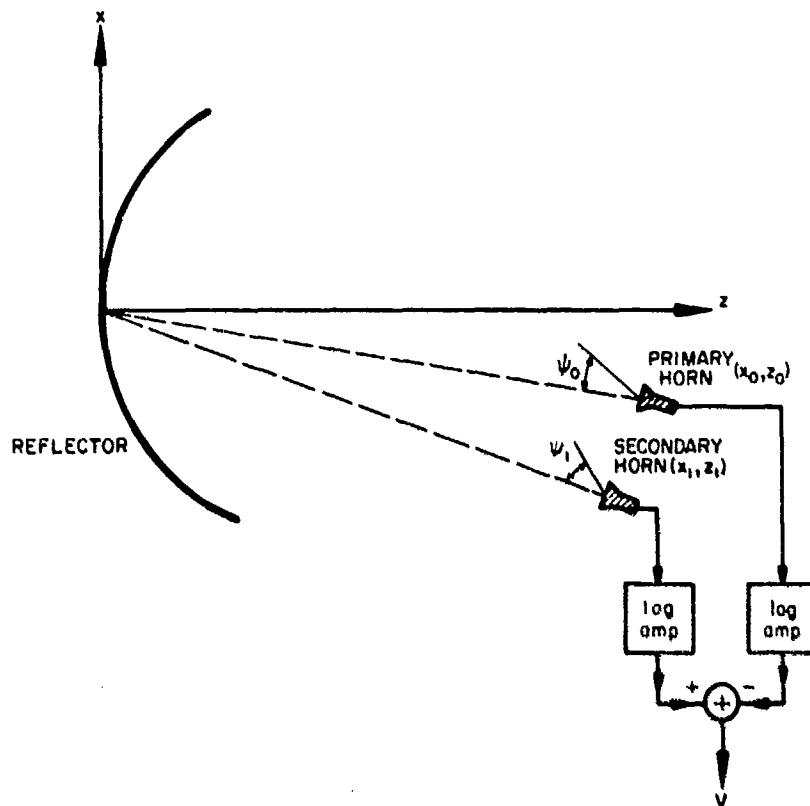


Figure 1. Modification of a Reflector Antenna so as to Obtain Altitude Information

$$V_0 = K \log_{10} \left[ \frac{r_1(\theta)}{r_0(\theta)} \right]^2 = K \log_{10} F(\theta), \quad (1)$$

where  $K$  is a constant and

$$F(\theta) = \left[ \frac{r_1(\theta)}{r_0(\theta)} \right]^2.$$

Then, neglecting system noise, we see that the target elevation angle  $\theta$  is

$$\theta = F^{-1} \left( \log_{10} \frac{V_0/K}{K} \right). \quad (2)$$

where  $F^{-1}$  is the inverse of the function  $F$ .

We have calculated the vacuum radiation pattern  $[r_0(\theta)]^2 = N_0(\theta)$  for the air search radar system. The results of our calculations are presented in Appendix A;

we show there that our computer calculations for the radiation pattern are in excellent agreement with the pattern measured using the actual air search reflector system. We have also performed calculations of the vacuum radiation pattern  $N_1 \equiv [f_1(\theta)]^2$  when only the secondary horn is excited. These results are presented in Appendix B for a number of different locations and types of secondary horn.

Next let us consider the effect of multipath on our ability to measure the target elevation  $\theta$ . If we refer to Figure 2 we see that the far field at the target (when multipath is included) due to the primary horn only is

$$E_0 = f_0(\theta) e^{i\phi_0(\theta)} + \rho D f_0(-\theta'') \exp \left\{ i\phi_0(-\theta'') + i k \Delta R \right\} \quad (3)$$

where  $\Delta R$  is the path difference between the direct and multipath ray,  $k$  is the signal wavenumber ( $2\pi/\lambda$ ),  $\rho$  is the reflection coefficient of the earth at the reflection point, and  $D$  is the spherical-earth dispersion factor. The field at the target due to the secondary horn is

$$E_1 = f_1(\theta) e^{i\phi_1(\theta)} + \rho D f_1(-\theta'') \exp \left\{ i\phi_1(-\theta'') + i k \Delta R \right\} \quad (4)$$

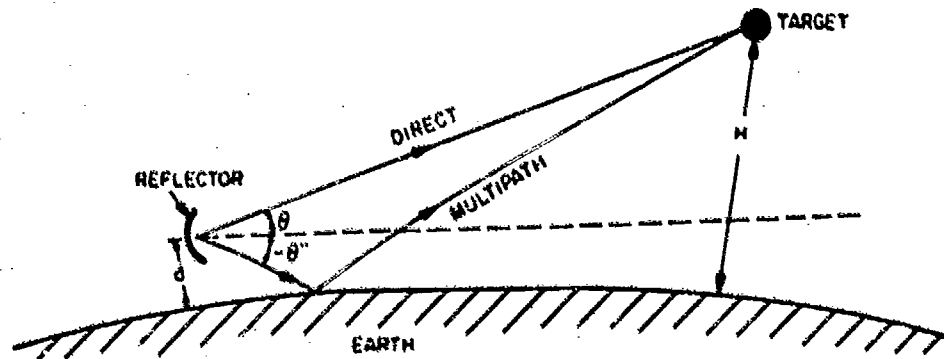


Figure 2. Geometry of the Direct and Multipath Links

By using Eqs. (3) and (4) along with Figure 1 it is clear that when multipath is included the output voltage  $V_M$  of the log-amps in Figure 1 is

$$\begin{aligned}
 V_M &= K \log_{10} \left| \frac{E_1}{E_0} \right|^2 \\
 &= K \log_{10} \left[ \frac{f_1(\theta)}{f_0(\theta)} \right]^2 + K \log_{10} \left[ \frac{1 + \rho D \frac{f_1(-\theta^*)}{f_1(\theta)} e^{i\psi_1}}{1 + \rho D \frac{f_0(-\theta^*)}{f_0(\theta)} e^{i\psi_0}} \right]^2
 \end{aligned} \tag{5}$$

where

$$\psi_0 \equiv \phi_0(-\theta^*) - \phi_0(\theta) + k \Delta R$$

and

$$\psi_1 \equiv \phi_1(-\theta^*) - \phi_1(\theta) + k \Delta R.$$

Upon comparing Eqs. (5) and (1) we see that

$$V_M = V_0 + \Delta V \tag{6}$$

where  $\Delta V$  is the error voltage due to the multipath, and is given by

$$\Delta V = K \log_{10} \left[ \frac{1 + \rho D \frac{f_1(-\theta^*)}{f_1(\theta)} e^{i\psi_1}}{1 + \rho D \frac{f_0(-\theta^*)}{f_0(\theta)} e^{i\psi_0}} \right]^2 \tag{7}$$

It is interesting to note from Eq. (7) that if the reflector design and horn locations are such that  $\psi_1 = \psi_0$  and

$$\frac{f_1(-\theta^*)}{f_1(\theta)} = \frac{f_0(-\theta^*)}{f_0(\theta)} \tag{8}$$

then from Eq. (7) we have  $\Delta V = 0$ , and the system operates precisely as it would if multipath were not present. In past analyses, authors have ignored the fact that  $\psi_0$  may not be equal to  $\psi_1$ . As we shall see in the next section,  $\psi_0 \neq \psi_1$  for the reflector system, and this leads to some interesting conclusions.

The error voltage given by Eq. (7) can be readily used to deduce an equivalent error in target altitude H. This error  $\Delta H$  is

$$\Delta H = \frac{\Delta V}{\left(\frac{\partial V_o}{\partial H}\right)_H} \quad (9)$$

where in Eq. (9) we replace  $\theta$  and  $\theta''$  by their definitions in terms of H. These are given by Eqs. (62) and (36) in Part 1 of this study.

We have now completed our theoretical review, and can begin to study some results computed using Eqs. (7) and (9) for the altitude error of a modified reflector. We will first consider only the error in altitude deduced on the basis of a single radar "hit", and will later consider the improvement (decrease in altitude error) which occurs when the altitudes deduced on multiple radar hits are averaged.

### 3. SINGLE-HIT ERRORS

In this section, we will present results for the altitude error, on the target altitude deduced from a single radar hit, for a modified radar system. As discussed previously, we are considering an antenna that is modified by adding a second horn in the focal region, as indicated in Figure 1. We shall present results for four different cases for the secondary horn pattern and location. These are tabulated in Table 1. The function  $F(\theta_1)$  is the radiation pattern of the secondary horn in the x-y plane, where  $g(\eta_1)$  is its pattern in the y-z plane ( $y$  is normal to the plane in Figure 1). The altitude error vs actual target altitude (for fixed range) for several of the cases tabulated in Table 1 are presented in Figures C1 to C4 in Appendix C. We note that the error is an oscillatory function of target altitude. The same is true of the plots of target altitude error vs target range (for fixed target altitude) shown in Figures C5 to C8 in Appendix C.

In this section we present the envelopes of the curves presented in Figures C1 to C4, and will label these envelopes as the "maximum altitude error". These results, for the cases listed in Table 1, are presented in Figures 3 to 6. Although we have presented the maximum error in target altitude as a function of actual target altitude H, one could also relate the error to the elevation angle  $\theta$ , by referring to Table 2. There are a number of observations we should make regarding the results presented in Figures 3 to 6. These are:

---

We have actually studied many more than four cases, but for conciseness we will present only those which are typical.

(a) The sharp peaks in altitude error in Figure 3 occur where  $d V_0/dH = 0$ . This means, that even in the absence of multipath there is likely to be a large error in target altitude (due to system noise).

(b) The worst altitude error (excluding those cases when  $d V_0/dH = 0$ ) occurs when the elevation angle  $\theta$  is about  $0.6^\circ$ . This point can be seen using Table 2 to relate the target altitude to  $\theta$ .

(c) The location and radiation pattern of the secondary horn can have a very significant effect on the magnitude of the maximum altitude error.

(d) The results in Figures 3 to 6 are rather insensitive to the height  $d$  of the reflector above the ground. Calculations for  $d = 0.01$  miles and  $d = 0.03$  miles gave substantially the same results as for  $d = 0.05$  miles, except very near to the horizon.

Table 1. Location and Pattern of the Secondary Horn

Case	$x_1$ (in.)	$z_1$ (in.)	$F(\psi_1)$	$g(\eta_1)$
A	-51.47	201.15	$1 - 4.92\psi_1^2 + 5.82\psi_1^4$	$\exp(-1.05\eta_1^2)$
B	-57.43	200.32	$\exp(-18.05\psi_1^2)$	"
C	-51.47	201.15	"	"
D	-55.63	200.589	1, 0	"

In addition to the aforementioned, there is another point which requires further detailed comment. The case labeled D in Table 1 and Figures 3 to 6 is one for which the primary and secondary radiation patterns very nearly fulfill the requirement expressed by Eq. (8). This can be seen by comparing Figure A1 in Appendix A with Figure B5 in Appendix B. Therefore why is the altitude error so large? The answer is that the phase  $\psi_1 = \psi_1(-\theta^*) - \psi_1(\theta) + k \Delta R$  does not equal  $\psi_0 = \psi_0(-\theta^*) - \psi_0(\theta) + k \Delta R$ . A comparison of the phase angle  $\psi_0(\theta)$  of the primary horn with  $\psi_1(\theta)$  of the secondary horn is shown in Figure 7. Because  $\psi_0(\theta)$  and  $\psi_1(\theta)$  are neither constants, nor linear functions of  $\theta$  with the same slope, it is clear that  $\psi_1(-\theta^*) - \psi_1(\theta)$  cannot equal  $\psi_0(-\theta^*) - \psi_0(\theta)$ ; consequently  $\psi_1 \neq \psi_0$ . Unfortunately, most analyses of monopulse reflector systems neglect the phase distribution of the radiated field. If the phase happens to be nearly linear over the range of  $\theta$  of interest this may not lead to incorrect results, but in general it does lead to incorrect results. In Figures 8 to 11 we have compared the results for the altitude error one would obtain by assuming  $\psi_1 = \psi_0$  with the correct results. For the case labeled B in Table 1 this assumption does not lead to radical differences, because the radiation patterns do not satisfy the requirement expressed by Eq. (8), but for Case D it is clear that the erroneous assumption that  $\psi_0 = \psi_1$  leads to completely

spurious results. Therefore the phase distribution of the radiated fields must be accurately included in any evaluation of a monopulse reflector system. Of course, we have included the phase angles  $\phi_0(\theta)$  and  $\phi_1(\theta)$  in all of our calculations.

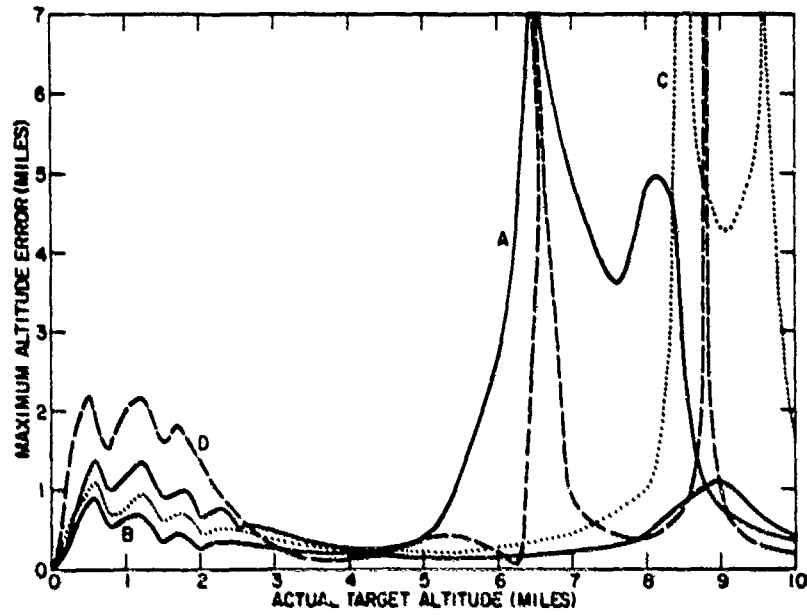


Figure 3. Maximum Altitude Error for Reflector Elevation,  $d = 0.05$  miles and Target Range,  $R = 50$  miles

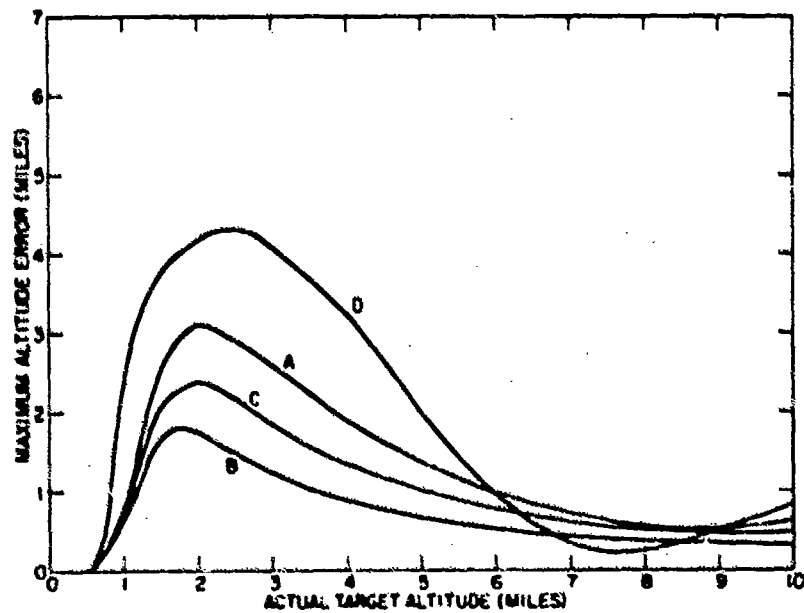


Figure 4. Maximum Altitude Error for Reflector Elevation,  $d = 0.05$  miles and Target Range,  $R = 100$  miles

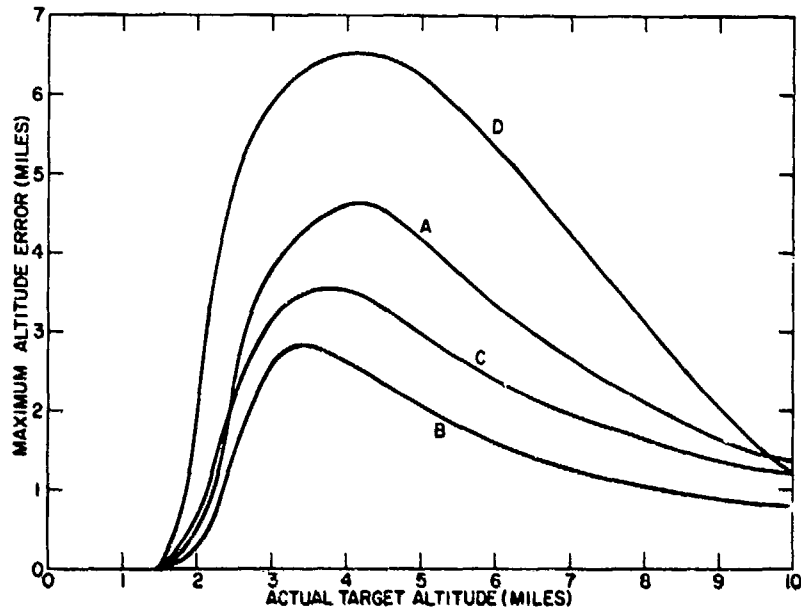


Figure 5. Maximum Altitude Error for Reflector Elevation,  $d = 0.05$  miles and Target Range,  $R = 150$  miles

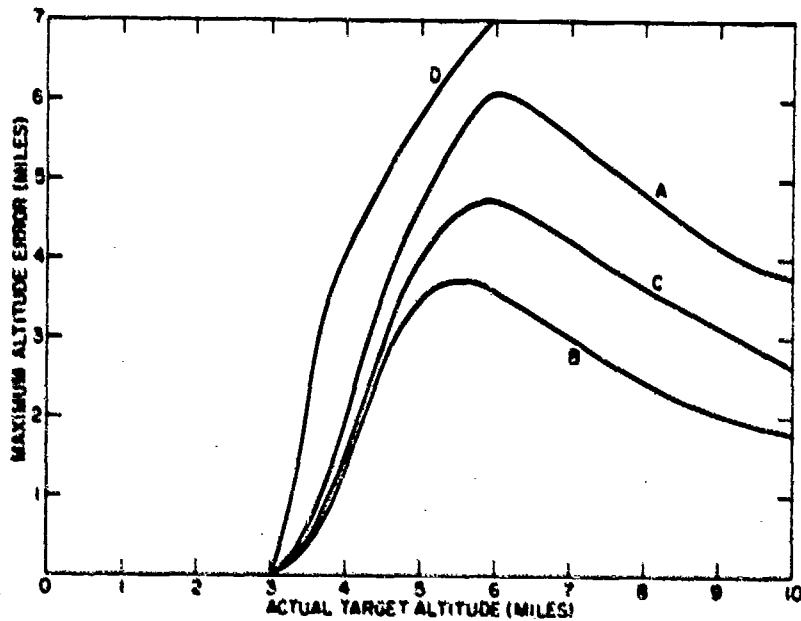


Figure 6. Maximum Altitude Error for Reflector Elevation,  $d = 0.05$  miles and Target Range,  $R = 200$  miles

Table 2. Relationship Between Altitude H and  $\theta$  for a Spherical Earth, and  $d = 0.05$  Miles

H (miles)	r = 200 miles $\theta$ (degrees)	R = 150 miles $\theta$ (degrees)	R = 100 miles $\theta$ (degrees)	R = 50 miles $\theta$ (degrees)
10	1.76	2.98	5.13	10.97
9	1.47	2.60	4.57	9.87
8	1.19	2.22	4.00	8.76
7	0.90	1.84	3.43	7.64
6	0.62	1.46	2.86	6.51
5	0.33	1.08	2.29	5.38
4	0.046	0.69	1.72	4.24
3	-0.240	0.31	1.15	3.10
2	below horizon	-0.069	0.57	1.96
1		below horizon	0.0017	0.82
0.5			below horizon	0.244

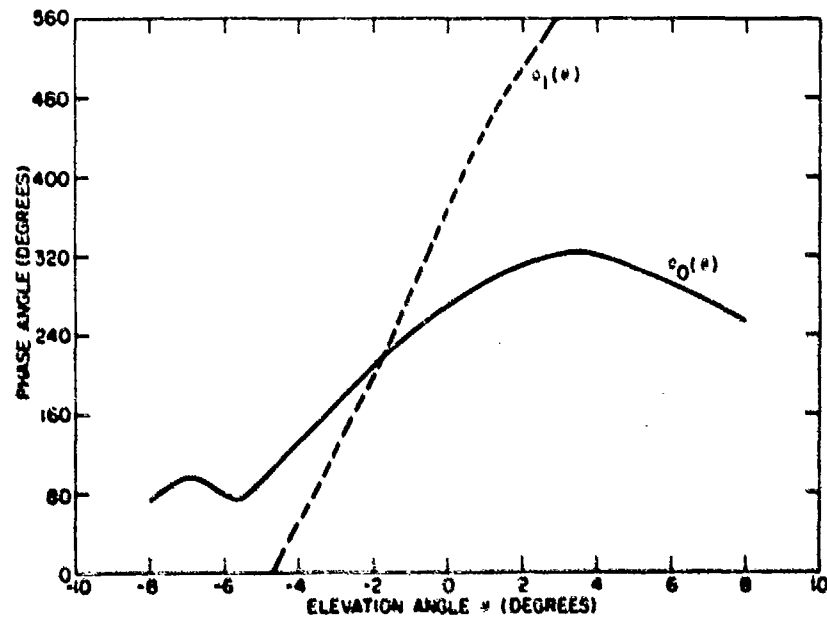


Figure 7. Phase Angle of the Radiation Field for the Primary Horn ( $\phi_0$ ) and the Secondary Horn ( $\phi_1$ ) for the Conditions of Case D of Table 1

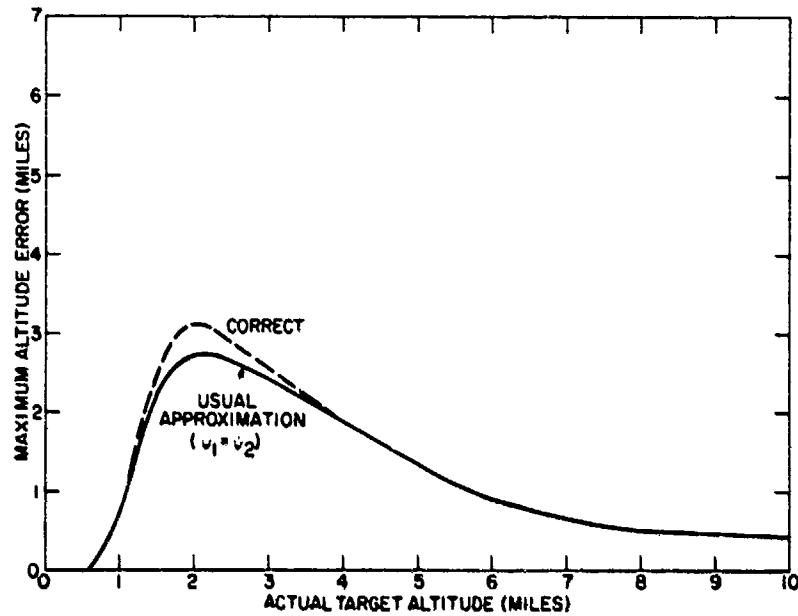


Figure 8. Effect of Using the Incorrect Assumption  $\psi_1 = \psi_2$  on the Maximum Altitude Error for the Reflector of Case A (Table 1) and  $R = 100$  miles,  $d = 0.05$  miles

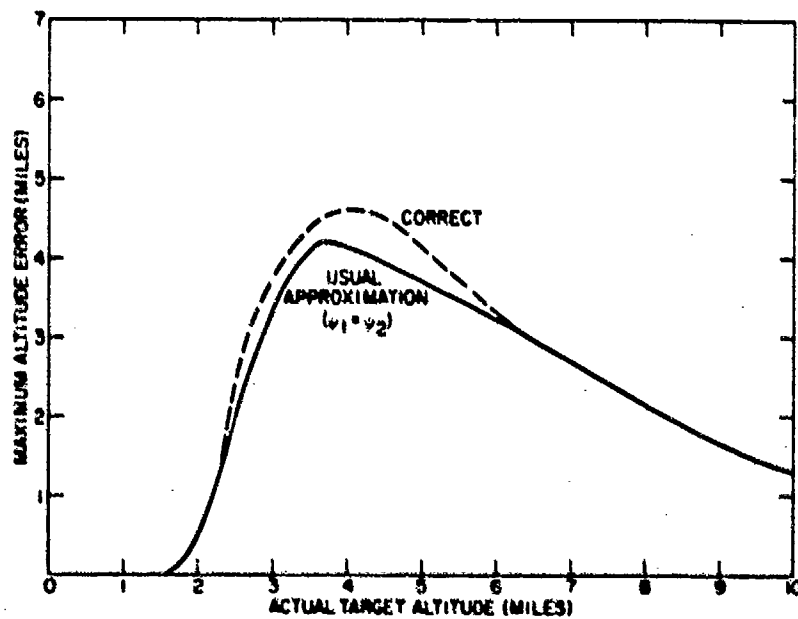


Figure 9. Effect of Using the Incorrect Assumption  $\psi_1 = \psi_2$  on the Maximum Altitude Error for the Reflector of Case A (Table 1) and  $R = 150$  miles,  $d = 0.05$  miles

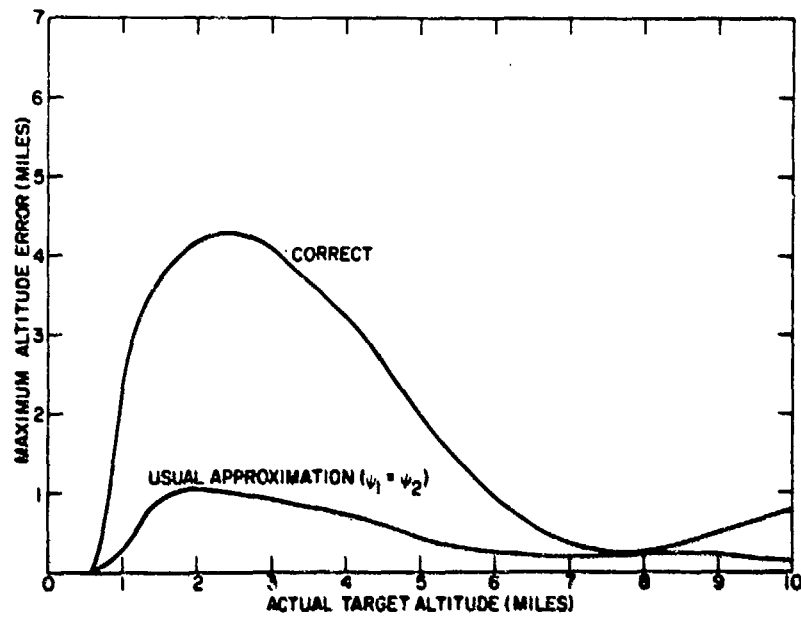


Figure 10. Effect of Using the Incorrect Assumption  $\epsilon_1 = \epsilon_2$  on the Maximum Altitude Error for the Reflector of Case D (Table 1) and  $R = 100$  Miles,  $d = 0.05$  Miles

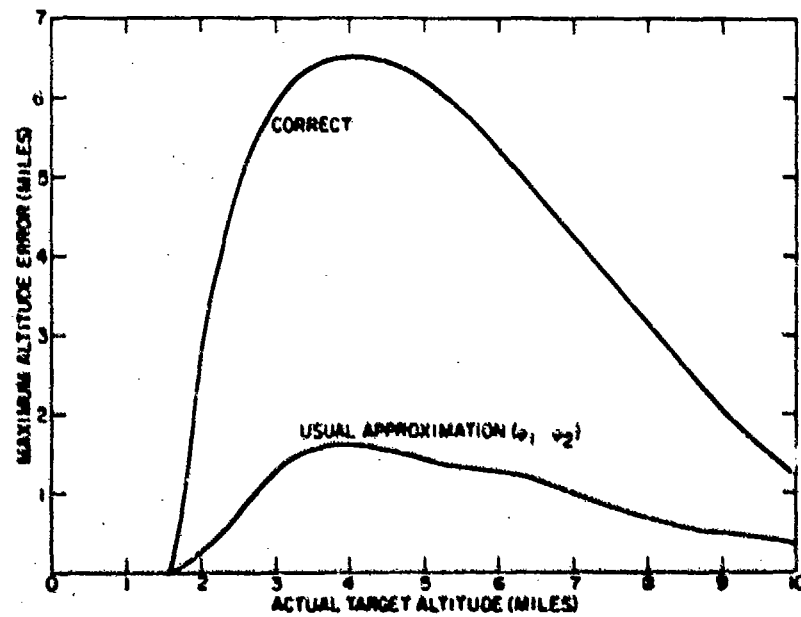


Figure 11. Effect of Using the Incorrect Assumption  $\epsilon_1 = \epsilon_2$  on the Maximum Altitude Error for the Reflector of Case D (Table 1) and  $R = 150$  Miles,  $d = 0.05$  Miles

#### 4. MULTIPLE-HIT ERRORS

Since the altitude errors for the modified radar system are reasonably large, as is clear from Figures 3 to 6, we inquire whether there is some way of processing the radar return so as to lessen the error in target altitude. One technique comes to mind when we observe Figures C5 to C8 in Appendix C. We observe that the altitude error is an oscillatory function of target range R. Consequently, if we sampled the error curve at a number of sufficiently widely spaced parts we would expect to reduce the error in our estimate of target altitude. The radar system scans at a rate such that there are six target hits per minute. For a target approaching the radar at 600 mph this means that there will be six hits for every ten miles of range covered by the target. We now suppose that the radar system estimates the target altitude on each of the six successive hits, and then averages these six values. Does this lead to a better estimate of true target altitude? The answer is yes! This can easily be seen by sampling the altitude error in Figure C5 of Appendix C at 6 equally spaced points (each point is 1.67 miles in range apart). Note that for some samples the altitude error is positive whereas for others it is negative, so that we expect that the altitude errors will decrease when we average in this fashion.

In order to be quantitative, let us consider six successive radar hits beginning at time  $t_0$  (for a target approaching at 600 miles per hour each hit will be 1.67 miles in range apart) and let us assume that the altitude error on each of these hits is  $\Delta H_i$  ( $i = 1, 6$ ). Then the average altitude error derived by averaging these 6 hits is

$$\Delta H(t_0) = \frac{1}{6} \sum_{i=1}^6 \Delta H_i. \quad (10)$$

However, the starting time  $t_0$  of our 6 pulse average can be arbitrary so we must also average over  $t_0$ . We denote this average by  $\langle \Delta H \rangle$ , and this is the average altitude error we are likely to have when we estimate the target altitude on the basis of a six hit average. Unfortunately, it is not sufficient to compute simply the average altitude error  $\langle \Delta H \rangle$ , because for situations such as shown in Figures C6 and C8 in Appendix C, the average altitude error  $\langle \Delta H \rangle$  is nearly zero, whereas a single sample average  $\Delta H(t_0)$  might differ greatly from zero, depending on the initial start  $t_0$  of the average. Therefore it is also necessary to compute the standard deviation of our average,  $\Delta H(t_0)$ . This is given by

$$\sigma_H = \left[ \langle \Delta H^2 \rangle - \langle \Delta H \rangle^2 \right]^{1/2}. \quad (11)$$

where  $\langle \rangle$  denotes an average over the initial time  $t_0$ . We can now define a maximum likely altitude error  $\epsilon_H$  as

$$\epsilon_H = \left| \langle \Delta H \rangle \right| + 2 \sigma_H. \quad (12)$$

This means that when we estimate the altitude by a 6 hit average as indicated in Eq. (10), there is only a 4 percent chance that the error will exceed  $\epsilon_H$ . In Figures 12 and 13 we have plotted this maximum likely error along with the error one would obtain on the basis of a single hit (no averaging). The values of  $\epsilon_H$  have been denoted by "averaged", and these have been plotted for three different reflector elevations,  $d = 0.01$  mile,  $d = 0.03$  mile and  $d = 0.77$  mile. From Figures 12 and 13 we note that averaging leads to significant reductions in altitude error, and consequently a much more accurate estimate of the actual altitude of the target.

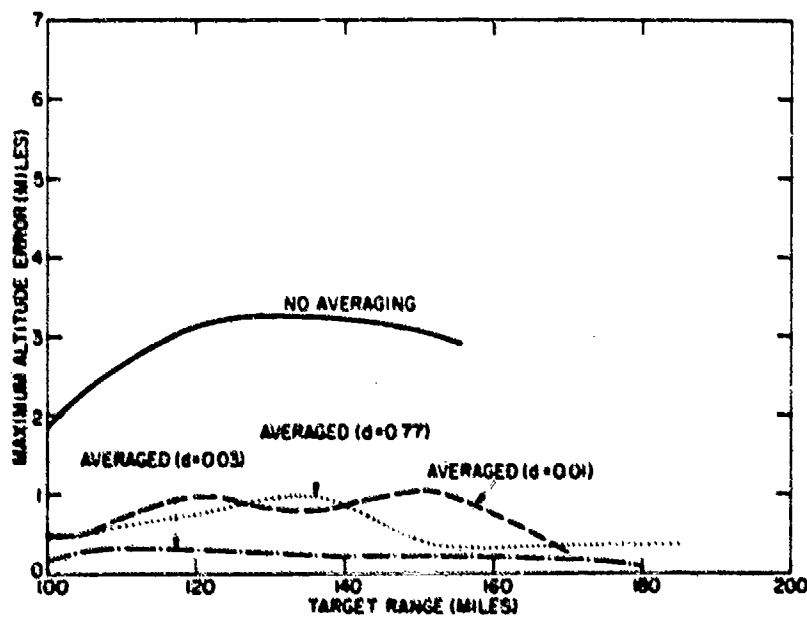


Figure 12. Effect of Averaging on the Maximum Altitude Error for a Target Flying at 3 Miles Altitude, for Case C of Table 1

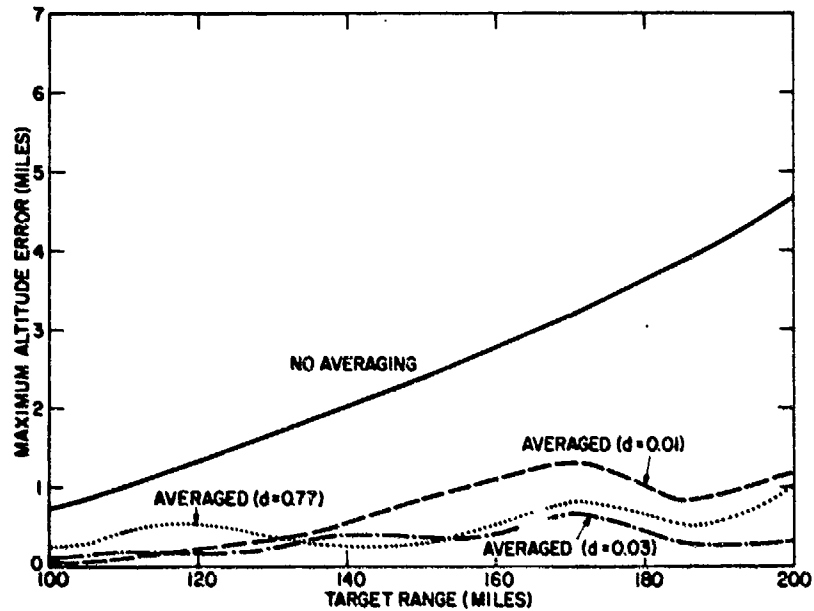


Figure 13. Effect of Averaging on the Maximum Altitude Error for a Target Flying at 6 Miles Altitude, for Case C of Table 1

### 5. CONCLUSIONS

- (a) The radiation pattern and location of the secondary feed horn can have a significant effect on the altitude error (due to multipath) of the modified radar.
- (b) One must be careful to properly include the reflector phase distribution,  $\phi(\theta)$ , in evaluating the altitude error due to multipath.
- (c) The error in altitude, or deduced on the basis of a single radar hit, can be reduced by a factor of 2 or more by averaging over a number of hits.

## Appendix A

### Element Pattern

We study here the radiation pattern of the reflector when fed by a single (primary) horn located in the focal region. This is the normal (non-monopulse) operating mode of the radar. We shall also assume here that the earth is absent, so that we will study the radiation pattern in the absence of multipath.

We have shown that the reflector of the air search radar can be modelled by the approximate analytical form (see Figure A1).

$$z = \alpha(x) + \beta(x) y^2 + \gamma(x) y^4 - 35.161 \quad (\text{A1})$$

where  $x, y, z$  are measured in inches and  $\alpha(x), \beta(x)$ , and  $\gamma(x)$  are given elsewhere. The coordinate  $y_a(x)$  describing the projection of the boundary of the dish (see Eq. (79) in Part 1) onto the  $z = 0$  plane is given elsewhere. The radiation pattern (see Part 1) of the feed horn can be approximated by

$$F(\theta_0) = 1 - 4.92 \theta_0^2 + 5.82 \theta_0^4 \quad (\text{A2})$$

$$g(\eta_0) = \exp - 1.6414 \eta_0^2 \quad (\text{A3})$$

where  $\theta_0$  is the angle (in radians) measured in the  $x' - z'$  plane in Figure 3 of Part 1, and  $\eta_0$  is the angle in radians in the  $y' - z'$  plane. The location of the primary feed horn is taken to be  $x = 34.0$  in.,  $y_0 = 0$ , and  $z_0 = 202.839$  in. and the assumed frequency of operation is 1350 MHz. A comparison of our theoretical radiation

pattern (obtained by using Eqs. (A1) to (A3) in Eq. (84) of Part 1) with experimental data is shown in Figure A1. It is quite evident that the agreement is excellent.

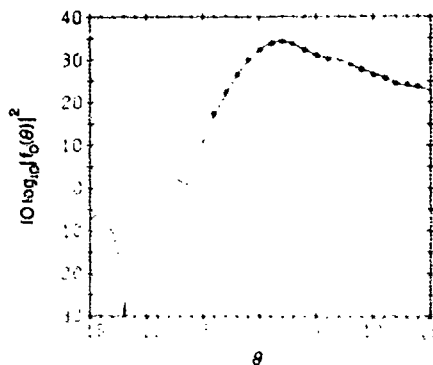


Figure A1. Radiation Pattern for the Reflector for the Case When the Primary Horn is Located at  $x_0 = 34.0$ ,  $y_0 = 0$ ,  $z_0 = 202.839$ . It is assumed that the secondary horn and the earth are absent. Computed results are indicated by the solid line and experimental values by  $\odot$

## **Appendix B**

### **Radiation Patterns for Various Types and Locations of the Secondary Horn**

In Figures B1 through B4 we show the radiation patterns of the air search radar (with the earth absent) when only the secondary horn is excited.

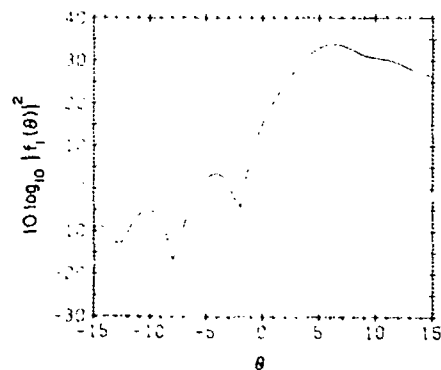


Figure B1. Radiation Pattern When the Secondary Horn is Located at  $x_1 = 51.47''$ ,  $z_1 = 201.15''$  and has  $F(\psi_1) = 1 - 4.92\psi_1^2 + 5.82\psi_1^4$  (denoted by Case A in Table 1)

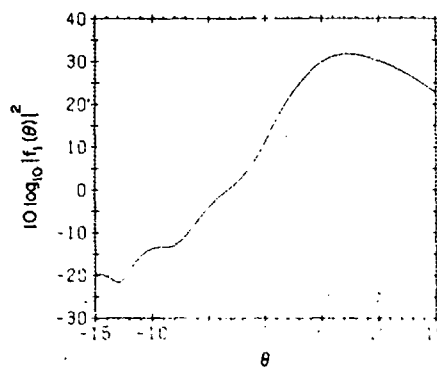


Figure B3. Radiation Pattern When the Secondary Horn is Located at  $x_1 = -51.47''$ ,  $z_1 = 201.15''$  and has  $F(\psi_1) = \exp(-18.05\psi_1^2)$ , (denoted by Case C in Table 1)

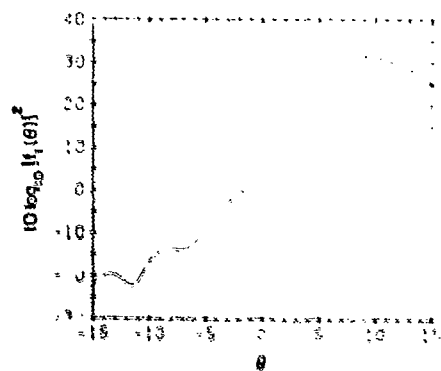


Figure B2. Radiation Pattern When the Secondary Horn is Located at  $x_1 = 57.43''$ ,  $z_1 = 200.32''$  and has  $F(\psi_1) = \exp(-18.05\psi_1^2)$ , (denoted by Case B in Table 1)

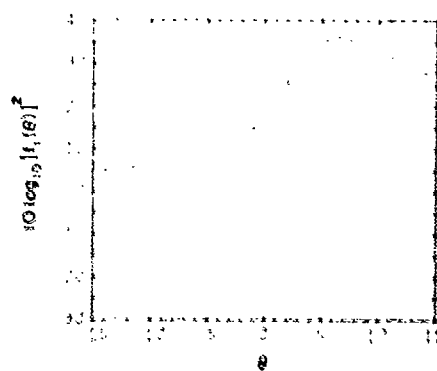


Figure B4. Radiation Pattern When the Secondary Horn is Located at  $x_1 = -55.63''$ ,  $z_1 = 200.589''$  and has  $F(\psi_1) = 1.0$  (denoted by Case D in Table 1)

## Appendix C

### Altitude Error Plots

In Figures C1 and C2 we show the computed altitude error vs target altitude for different secondary horn locations when the target range is 100 miles. In Figures C3 and C4 we show the computed altitude error vs target altitude when the range is 150 miles. Figures C5 to C8 show the altitude error vs range when the target flies at a constant altitude, for several different radar dish elevations. In all of these results we have considered only specular reflections from the earth's surface.

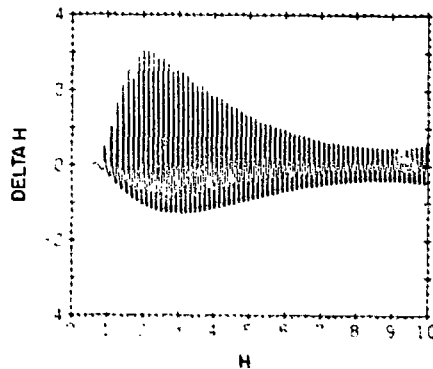


Figure C1. Altitude Error (miles) vs Altitude (miles) for a Target Range of 100 Miles. Also,  $d = 0.05$  miles and the reflector system is given by Case A in Table 1

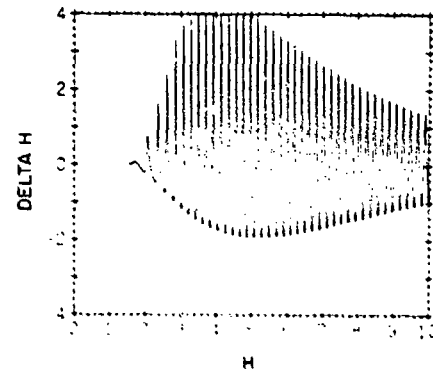


Figure C3. Altitude Error (miles) vs Altitude (miles) for 150 Mile Target Range. Also,  $d = 0.05$  miles and reflector system is given by Case A in Table 1

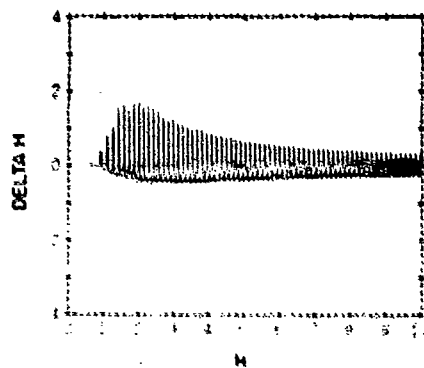


Figure C2. Altitude Error (miles) vs Altitudes (miles) for 100 Mile Target Range. Also,  $d = 0.05$  miles and reflector system is given by Case B in Table 1

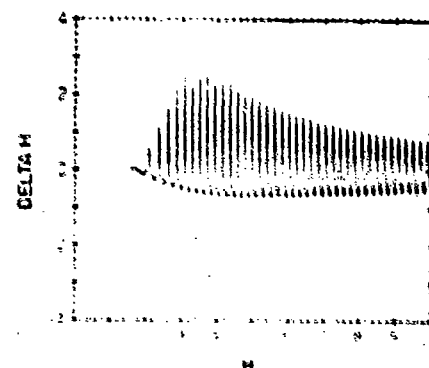


Figure C4. Altitude Error (miles) vs Altitude (miles) for 150 Mile Target Range. Also,  $d = 0.05$  miles and reflector system is given by Case B in Table 1

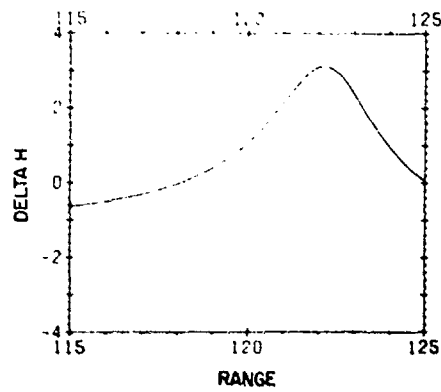


Figure C5. Altitude Error (miles) vs Range (miles) for a Target Altitude of 3 Miles and Reflector Elevation  $d = 0.01$  Miles (52'), Assuming the Reflector System of Case C in Table 1

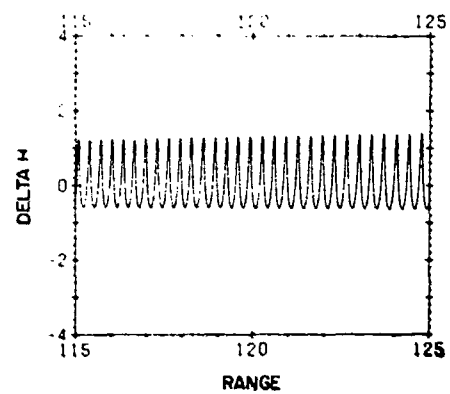


Figure C7. Altitude Error (miles) vs Range (miles) for a Target Altitude of 3 Miles and a Reflector Elevation  $d = 0.76$  Miles (4000'), Assuming the Reflector System of Case C in Table 1

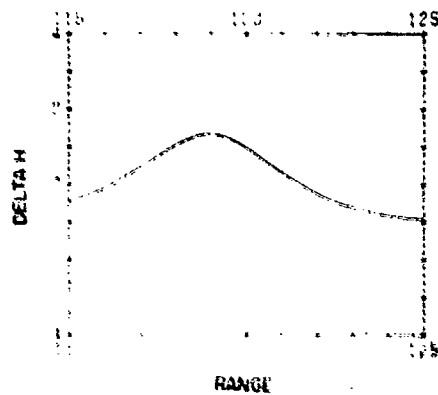


Figure C6. Altitude Error (miles) vs Range (miles) for a Target Altitude of 6 Miles and a Reflector Elevation  $d = 0.01$  Miles (52'), Assuming the Reflector System of Case C in Table 1

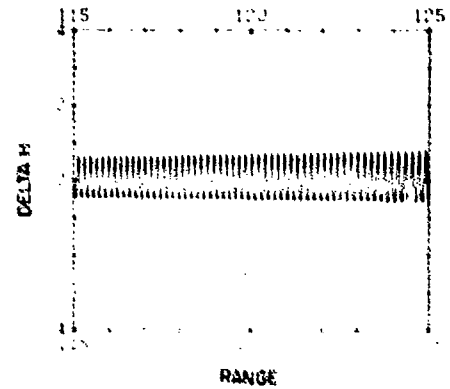


Figure C8. Altitude Error (miles) vs Range (miles) for a Target Altitude of 6 Miles and a Reflector Elevation  $d = 0.76$  Miles (4000'), Assuming the Reflector System of Case C in Table 1

*MISSION  
of  
Rome Air Development Center*

*RADC plans and conducts research, exploratory and advanced development programs in command, control, and communications (C<sup>3</sup>) activities, and in the C<sup>3</sup> areas of information sciences and intelligence. The principal technical mission areas are communications, electromagnetic guidance and control, surveillance of ground and aerospace objects, intelligence data collection and handling, information system technology, ionospheric propagation, solid state sciences, microwave physics and electronic reliability, maintainability and compatibility.*

